Geoscience Frontiers 5 (2014) 515–523

Contents lists available at ScienceDirect

China University of Geosciences (Beijing)

Geoscience Frontiers

journal homepage: www.elsevier.com/locate/gsf

Research paper

Dating of zircon from high-grade rocks: Which is the most reliable method?

Alfred Kröner[a,*], Yusheng Wan[a], Xiaoming Liu[b], Dunyi Liu[a]

[a] Beijing SHRIMP Centre, Institute of Geology, Chinese Academy of Geological Sciences, 26 Baiwanzhuang Road, 100037 Beijing, China
[b] State Key Laboratory of Continental Dynamics, Department of Geology, Northwest University, Xi'an 710069, China

A R T I C L E I N F O

Article history:
Received 19 January 2014
Received in revised form
18 March 2014
Accepted 20 March 2014
Available online 13 April 2014

Keywords:
Zircon dating
High-grade rock
SHRIMP
LA-ICP-MS

A B S T R A C T

Magmatic zircon in high-grade metamorphic rocks is often characterized by complex textures as revealed by cathodoluminenscence (CL) that result from multiple episodes of recrystallization, overgrowth, Pb-loss and modifications through fluid-induced disturbances of the crystal structure and the original U-Th-Pb isotopic systematics. Many of these features can be recognized in 2-dimensional CL images, and isotopic analysis of such domains using a high resolution ion-microprobe with only shallow penetration of the zircon surface may be able to reconstruct much of the magmatic and complex post-magmatic history of such grains. In particular it is generally possible to find original magmatic domains yielding concordant ages. In contrast, destructive techniques such as LA-ICP-MS consume a large volume, leave a deep crater in the target grain, and often sample heterogeneous domains that are not visible and thus often yield discordant results which are difficult to interpret. We provide examples of complex magmatic zircon from a southern Indian granulite terrane where SHRIMP II and LA-ICP-MS analyses are compared. The SHRIMP data are shown to be more precise and reliable, and we caution against the use of LA-ICP-MS in deciphering the chronology of complex zircons from high-grade terranes.

1. Introduction

Zircon dating by quadrupole LA-ICP-MS has become a common and widespread practice, and large numbers of analyses have been produced in recent years due to the short time required for each analysis and the growing number of zircon geochronology laboratories. This technique has proved reliable in dating relatively simple magmatic rocks with homogeneous zircon populations and has proved most effective in the dating of detrital zircon grains where high precision is not required.

The main challenge for LA-ICP-MS analysis is a reliable correction for common Pb, due to the presence of mercury in the argon gas used in many laboratories to produce the plasma that causes an isobaric interference by ^{204}Hg on ^{204}Pb (e.g., Andersen, 2002). Such correction is particularly important for samples with low ^{206}Pb/^{204}Pb ratios. Different methods were developed to overcome this problem (e.g., Horn et al., 2000; Košler et al., 2002; Jackson et al., 2004; Gehrels et al., 2008; Cottle et al., 2009), but most users simply make no correction, assuming that zircon has no or only insignificant common Pb. However, this is often not the case for early Precambrian zircon with a complex history (e.g., Table 4 in Kröner et al., 1989). Alternatively, some users correct for common Pb with a model calculation that assumes a coherent behaviour of Th/Pb and U/Pb and estimates the time of the isotopic disturbance (Andersen, 2002). The crater produced in the zircon by laser ablation, depending on the laser energy density (normally 5–6 Hz and 100 mJ), and assuming about 25–30 pulses during a single analysis, is about 35–40 μm deep (Figs. 1 and 2), thus the technique is rather destructive and, as further discussed below, the deep pit is likely to analyze isotopically inhomogeneous domains in zircon with complex histories. On the other hand, isotopically simple magmatic or metamorphic zircon can be analyzed fast and with high precision due to the large volume ablated.

An alternative, but more expensive and much more time-consuming technique is dating of small zircon domains by a sensitive high-resolution ion microprobe such as SHRIMP II or Cameca

* Corresponding author.
E-mail address: kroener@uni-mainz.de (A. Kröner).

Peer-review under responsibility of China University of Geosciences (Beijing)

Production and hosting by Elsevier

1674-9871/$ – see front matter
http://dx.doi.org/10.1016/j.gsf.2014.03.012

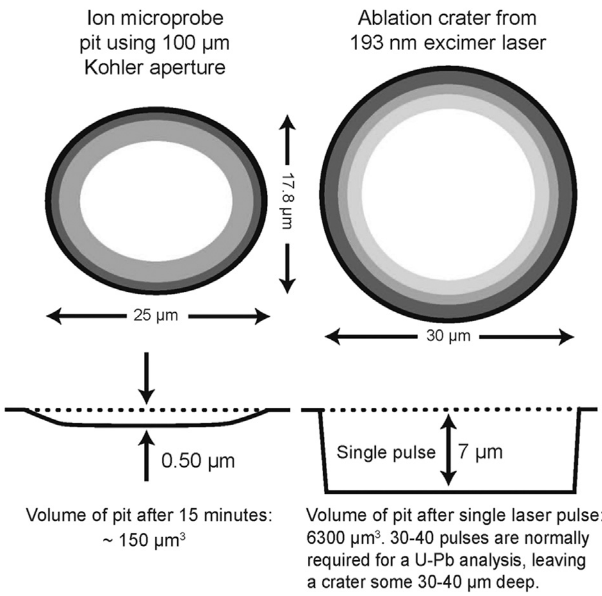

Figure 1. Size of a typical pit produced in zircon by using an ion microprobe during a 15 min analytical run (five cycles) (left) compared to the size of an ablation crater made from about 10 pulses of an excimer laser (right). Bottom drawings show generalized cross-sections of the excavations made by the two techniques (modified from Patchett and Samson, 2011).

1280. The advantage of this technique is the shallow analytical pit, only 1.5–2 μm deep (based on Lee et al., 1997, see Figs. 1 and 2), and the ability to precisely correct for common Pb, whereas the estimate of total U is less precise than using ICP-MS.

Zircon populations from rocks with long and multiphase tectono-metamorphic histories generally do not consist of homogeneous crystals but may contain multiple components such as old cores, surrounded by magmatic overgrowth and further surrounded by metamorphic overgrowth. However, the robustness of zircon without radiation damage, even during ultra-high temperature metamorphism, and the insignificance of Pb-diffusion have been demonstrated in many studies, and careful CL- and trace element-assisted investigations make it possible to extract reliable age data from such grains (e.g., Möller et al., 2003; Kooijman et al., 2011). In contrast, fluid-induced alteration is common in high-grade metamorphic terranes (e.g., Geisler et al., 2007; Flowers et al., 2010; Wan et al., 2011; Dong et al., 2013; Ma et al., 2012), and recrystallization, combined with Pb-loss, will produce variable discordance in a zircon population, particularly in granulite-facies assemblages (e.g., Corfu, 2013; Kröner et al., 2013). Fig. 3 provides two examples of complex zircon showing evidence of recrystallization within small domains.

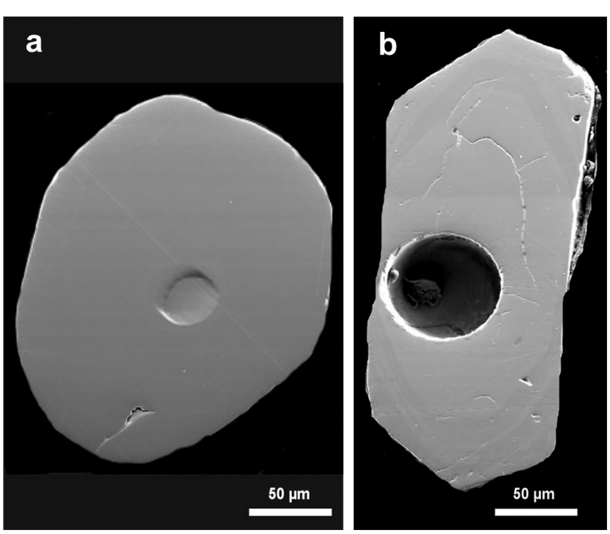

Figure 2. (a) SHRIMP II pit on metamorphic zircon as seen in back-scattered electron (BSE) image; (b) laser pit in BSE image produced after LA-ICP-MS analysis.

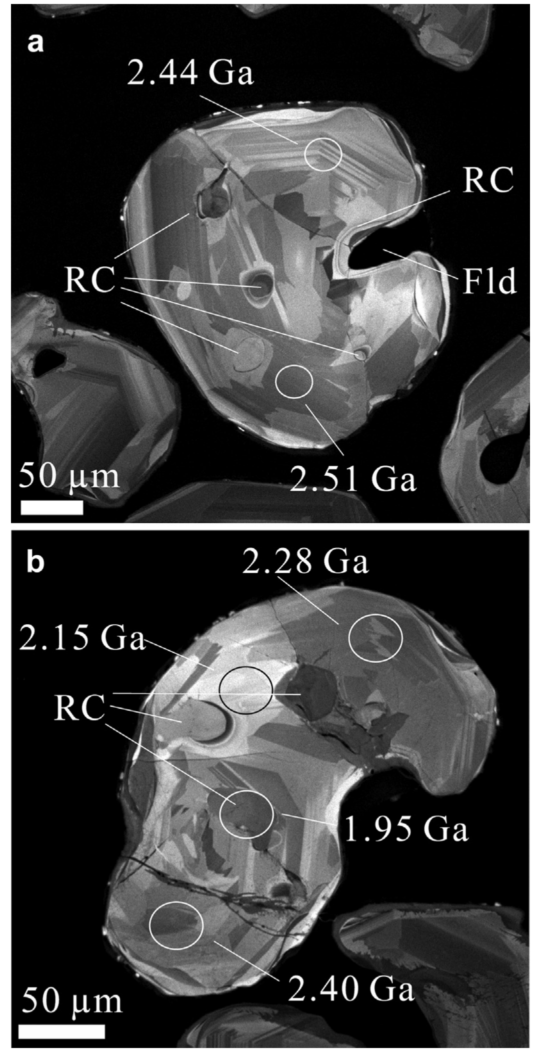

Figure 3. Cathodoluminescence images for zircons from a cpx- and opx-bearing metadiorite gneiss of the high-grade late Archaean terrane in eastern Shandong, North China craton (Wan et al., 2011). These zircons show banded, fir-tree, sector- and/or oscillatory zoning. Positions of SHRIMP II analytical sites with ages (in Ga) are indicated. Note strong luminescence in small, local domains, probably due to recrystallization (RC). Palaeoproterozoic high-grade metamorphism at ca. 1.95 Ga (dark grey, recrystallized domains in a and b) has caused strong recrystallization of magmatic zircon (2.51 Ga, see b) and the formation of new metamorphic domains (b). Ages between 1.95 and 2.51 are due to mixing of igneous and metamorphic components.

More severely discordant data are generally the result of either Pb-loss or mixing of two different zircon phases. Solid state diffusion of Pb from zircon is extremely slow and unlikely to be effective at normal crustal temperatures (Mezger and Krogstad, 1997; Cherniak and Watson, 2001). Therefore, Pb-loss occurs either by extraction of Pb from altered domains by fluids (e.g., Krogh and Davis, 1974, 1975) or by expulsion and/or intragrain redistribution of Pb during recrystallization (e.g., Pidgeon et al., 1998; Connelly, 2001; McFarlane et al., 2005). The former mechanism generally

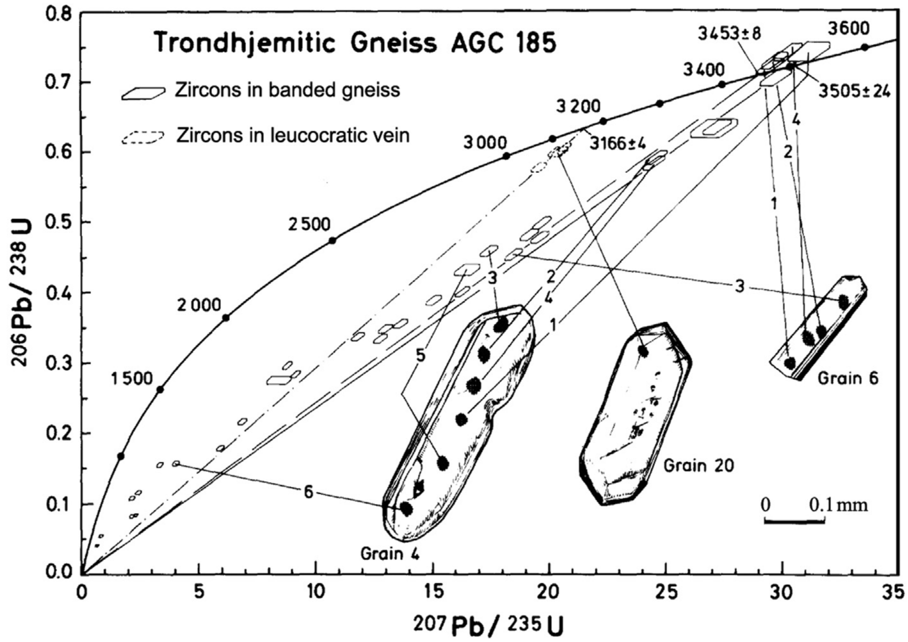

Figure 4. Concordia diagram showing SHRIMP I zircon analyses from trondhjemitic gneiss of the Ancient Gneiss Complex in northeast Swaziland. Note large variation in isotopic ratios shown by 6 analytical spots within grain 4 (reproduced from Kröner et al., 1989).

implies the parallel existence of concordant and discordant domains, as is often observed in high-resolution ion-microprobe analyses (Fig. 4), and thus concordant or near-concordant ages can be obtained.

In contrast, Pb-loss by recrystallization and/or redistribution, particularly under fluid conditions, often leads to partial or even complete isotopic resetting and no closed-system domains remain that can provide concordant ages. Reverse discordance, as

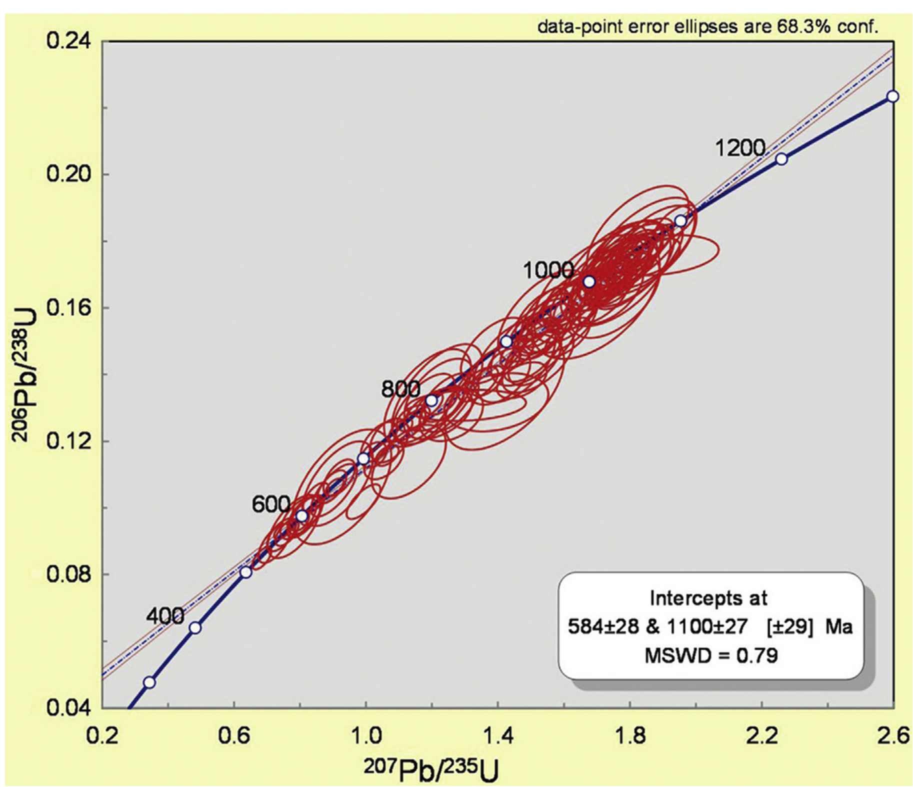

Figure 5. Concordia diagram showing LA-ICP-MS analytical data for zircons from granulite-facies Vijayan Complex, southeastern Sri Lanka. Error ellipses are 68.3% confidence. Note excellent linear distribution of isotopic ratios and two mean concordia intercept ages at 1100 ± 28 and 584 ± 28 Ma that define the maximum age of Vijayan magmatism and the peak of high-grade metamorphism as defined by both SHRIMP II and LA-ICP-MS dating (from Kröner et al., 2013).

Table 1
SHRIMP II analytical data for zircon from two charnockite samples of the Nagercoil Complex, southernmost India.

Sample No.	U (ppm)	Th (ppm)	$^{206}Pb/^{204}Pb$	$^{208}Pb/^{206}Pb$	$^{207}Pb/^{206}Pb$	$^{206}Pb/^{238}U$	$^{207}Pb/^{235}U$	$^{206}Pb/^{238}U$ age ± 1σ (Ma)	$^{207}Pb/^{235}U$ age ± 1σ (Ma)	$^{207}Pb/^{206}Pb$ age ± 1σ (Ma)
NGB-1B-1	1046	249	119,474	0.0712 ± 4	0.1206 ± 3	0.2830 ± 34	4.707 ± 59	1606 ± 17	1768 ± 10	1965 ± 4
NGB-1B-2	524	164	83,056	0.0841 ± 6	0.1121 ± 4	0.2173 ± 26	3.359 ± 43	1268 ± 14	1495 ± 10	1834 ± 6
NGB-1B-3	983	256	78,247	0.0746 ± 4	0.1222 ± 3	0.2925 ± 35	4.928 ± 61	1654 ± 17	1807 ± 11	1989 ± 4
NGB-1B-4	393	129	32,436	0.0955 ± 6	0.1282 ± 4	0.3753 ± 45	6.631 ± 85	2054 ± 21	2064 ± 11	2073 ± 6
NGB-1B-5	553	182	50,327	0.0936 ± 4	0.1285 ± 3	0.3805 ± 46	6.742 ± 85	2079 ± 21	2078 ± 11	2077 ± 4
NGB-1B-6	218	55	133,156	0.0655 ± 8	0.1286 ± 5	0.3848 ± 47	6.822 ± 92	2099 ± 22	2089 ± 12	2079 ± 7
TB1-1	833	199	83,893	0.0677 ± 3	0.1251 ± 3	0.3268 ± 39	5.635 ± 70	1823 ± 19	1921 ± 11	2030 ± 4
TB1-2	409	325	30,675	0.2238 ± 8	0.1283 ± 4	0.3705 ± 45	6.555 ± 84	2032 ± 21	2053 ± 11	2075 ± 5
TB1-3	310	206	62,461	0.1953 ± 10	0.1247 ± 4	0.3182 ± 38	5.471 ± 72	1781 ± 19	1896 ± 11	2025 ± 7
TB1-4	210	123	42,230	0.1655 ± 11	0.1282 ± 6	0.3773 ± 46	6.670 ± 90	2064 ± 22	2069 ± 12	2073 ± 8
TB1-5	300	156	34,211	0.1467 ± 9	0.1269 ± 5	0.3482 ± 42	6.091 ± 80	1926 ± 20	1989 ± 11	2055 ± 7
TB1-6	296	164	46,948	0.1503 ± 8	0.1284 ± 4	0.3840 ± 47	6.797 ± 89	2095 ± 22	2085 ± 12	2076 ± 6
TB1-7	222	74	32,520	0.0976 ± 9	0.1283 ± 6	0.3769 ± 46	6.668 ± 90	2062 ± 22	2068 ± 12	2075 ± 8
TB1-8	32	46	989	0.4400 ± 190	0.0598 ± 70	0.0910 ± 13	0.750 ± 90	561 ± 8	568 ± 52	595 ± 255

Note: NGB-1A-1 is spot on grain 1, NGB-1A-2 is spot on grain 2, etc.

occasionally observed in ion-microprobe analyses (e.g., Williams et al., 1984) and more rarely in ICP-MS data (e.g., Xia et al., 2004), may be due to within-grain redistribution (e.g., Kusiak et al., 2013) or incorrect assessment of U/Pb calibration. These cases are typical of high-grade metamorphic terranes where only discordant data can be extracted from many zircons (e.g., Corfu et al., 1994; Connelly, 2001; Moser et al., 2011). Such severe partial resetting by recrystallization and associated new growth results in linear arrays of data points in the concordia diagram between the time of crystallization and that of secondary reworking and/or local new growth (Moser et al., 2009; Kröner et al., 2013; see Fig. 5).

A further problem related to zircon discordance concerns the interpretation of data that are nearly, but not fully, concordant, and this is discussed in detail by Corfu (2013). In many cases the slight discordance is due to ancient Pb-loss, and the ages can then be extrapolated by projecting a line through the data from lower-intercept ages corresponding to the time of the supposed event (see Fig. 5). However, such events are often not evident from geological considerations, and such upper intercept extrapolations may thus be erroneous. In cases where the difference between the two concordia intercept ages is relatively small, the discordia line becomes subparallel to the concordia curve and, dependent on the magnitude of the uncertainty, indistinguishable from it (e.g., Corfu et al., 1994; Corfu, 2007; Kröner et al., 2013; see Fig. 5).

Such a case is demonstrated in Fig. 5 where LA-ICP-MS data for zircons from granulite-facies gneisses in southeastern Sri Lanka plot between the igneous emplacement age at ca. 1100 Ma and a severe high-grade metamorphic event at 580 Ma (Kröner et al., 2013). If these two events were not known, the data could easily be interpreted as reflecting concordant ages implying multiple growth periods, and the possibility that individual subconcordant data may be recording partial resetting or mixing is not always considered. The zircon isotopic systematics reported by Ashwal et al. (1999) from a leuconorite in southwestern Madagascar illustrate this point. These authors reported quasi-concordant zircon analyses with ages between 631 and 549 Ma (Ashwal et al., 1999, their Fig. 1) and conclude that these U-Pb ages are indicative of high-temperature Pb-loss during one or more protracted periods of granulite-facies metamorphism with minor episodic or continuous metamorphic zircon growth during a long-lasting (ca. 80 Ma) high-grade metamorphic event. Such interpretation is highly implausible since thermal considerations make it unlikely that the lower crust can maintain a constant high temperature of >800 °C for this long period of time. It is more likely that the data are slightly discordant and follow a discordia line almost indistinguishable from the concordia curve between a

Table 2
LA-ICP-MS analytical data for zircon from two charnockite samples of the Nagercoil Complex, southernmost India.

Sample No. and spot*	^{238}U (ppm)	^{232}Th (ppm)	$^{206}Pb/^{204}Pb$	$^{207}Pb/^{206}Pb$	$^{206}Pb/^{238}U$	$^{207}Pb/^{235}U$	$^{206}Pb/^{238}U$ age ± 1σ (Ma)	$^{207}Pb/^{235}U$ age ± 1σ (Ma)	$^{207}Pb/^{206}Pb$ age ± 1σ (Ma)
NGB1-1	912	125	5473	0.1126 ± 11	0.2053 ± 10	3.188 ± 16	1204 ± 5	1454 ± 4	1842 ± 19
NGB1-2	231	90	1719	0.0953 ± 10	0.1568 ± 8	2.062 ± 13	939 ± 5	1136 ± 4	1535 ± 20
NGB1-3	269	79	10,887	0.1204 ± 12	0.3249 ± 16	5.395 ± 29	1813 ± 8	1884 ± 5	1963 ± 18
NGB1-4	369	106	7578	0.1268 ± 13	0.3278 ± 16	5.731 ± 30	1828 ± 8	1936 ± 5	2054 ± 18
NGB1-5	2300	155	10,822	0.1063 ± 11	0.1548 ± 8	2.269 ± 11	928 ± 4	1203 ± 4	1737 ± 18
NGB1-6	474	143	9101	0.1221 ± 12	0.2668 ± 13	4.492 ± 23	1524 ± 7	1730 ± 4	1988 ± 18
NGB1-7	242	69	2128	0.1155 ± 13	0.2350 ± 13	3.742 ± 26	1841 ± 8	1581 ± 6	1888 ± 20
NGB1-8	615	170	12,857	0.1273 ± 13	0.3306 ± 16	5.801 ± 29	1019 ± 5	1947 ± 4	2061 ± 18
NGB1-9	240	76	4636	0.1008 ± 12	0.1713 ± 9	2.382 ± 17	1964 6	1237 ± 5	1640 ± 21
TB1-1	217	68	3586	0.1169 ± 13	0.2462 ± 13	3.972 ± 25	1419 ± 7	1628 ± 5	1910 ± 19
TB1-2	400	361	14,484	0.1364 ± 14	0.3239 ± 16	6.092 ± 33	1809 ± 8	1989 ± 5	2181 ± 18
TB1-3	349	194	12,451	0.1306 ± 13	0.3190 ± 16	5748 ± 30	1785 ± 8	1939 ± 5	2106 ± 18
TB1-4	1539	148	3821	0.1350 ± 14	0.2811 ± 14	5.235 ± 26	1597 ± 7	1858 ± 4	2164 ± 17
TB1-5	947	207	3908	0.1277 ± 13	0.2787 ± 14	4.909 ± 25	1585 ± 7	1804 ± 4	2066 ± 18
TB1-6	405	14.2	2471	0.0646 ± 8	0.1030 ± 6	0.918 ± 8	632 ± 3	661 ± 4	760 ± 27
TB1-7	750	39.3	2700	0.0640 ± 7	0.0929 ± 5	0.821 ± 6	573 ± 3	609 ± 3	743 ± 24
TB1-8	72	51	710	0.0632 ± 9	0.0883 ± 5	0.769 ± 8	546 ± 3	580 ± 5	714 ± 29
TB1-9	250	162	11,730	0.1255 ± 13	0.3728 ± 19	6.456 ± 36	2043 ± 9	2040 ± 5	2036 ± 18
TB1-10	454	128	13,468	0.1315 ± 13	0.3243 ± 16	5.883 ± 30	1811 ± 8	1959 ± 4	2118 ± 18

Note: *NGB1-1 is spot on grain 1, NGB1-2 is spot on grain 2, etc.

Figure 6. CL-images of zircons with complex internal textures from high-grade charnockitic gneisses of southern India. For explanation see text. RC – recrystallized domain; Fl – fluid-induced recrystallization.

likely igneous emplacement event for the leuconorite at 631 Ma and high-grade metamorphism at ca. 550 Ma. This metamorphic event is widespread in Madagascar and neighbouring high-grade areas of Sri Lanka and southern India that were all part of East Gondwana during the Pan-African event (Kröner, 2001; Collins et al., 2014).

Data such as reported by Ashwal et al. (1999) and those shown in Fig. 4 demonstrate Pb-loss or recrystallization, and since a precise correction for common Pb cannot be made for LA-ICP-MS data, it is often impossible to decide whether a particular analysis is concordant or slightly discordant. This is most relevant for Phanerozoic to Neoproterozoic zircons where it is customary to report $^{206}Pb/^{238}U$ ages. Such ages, if the data are discordant, are geologically questionable and almost always too low. This analytical problem can be overcome if different spots on a specific grain or several grains from the same sample are analyzed because it is unlikely that all grins or grain-domains contain the same amount of common Pb or experienced the same amount of Pb-loss.

2. Comparative SHRIMP II and LA-ICP-MS isotopic data for zircons with complicated internal textures from the high-grade terrane of southern India

We present examples of complicated zircons from a high-grade terrane in southern India as shown by their cathodoluminescence (CL) images that have been dated by both SHRIMP II and LA-ICP-MS techniques. The analytical procedures are summarized in the Appendix. Zircons were extracted from charnockitic gneisses of the

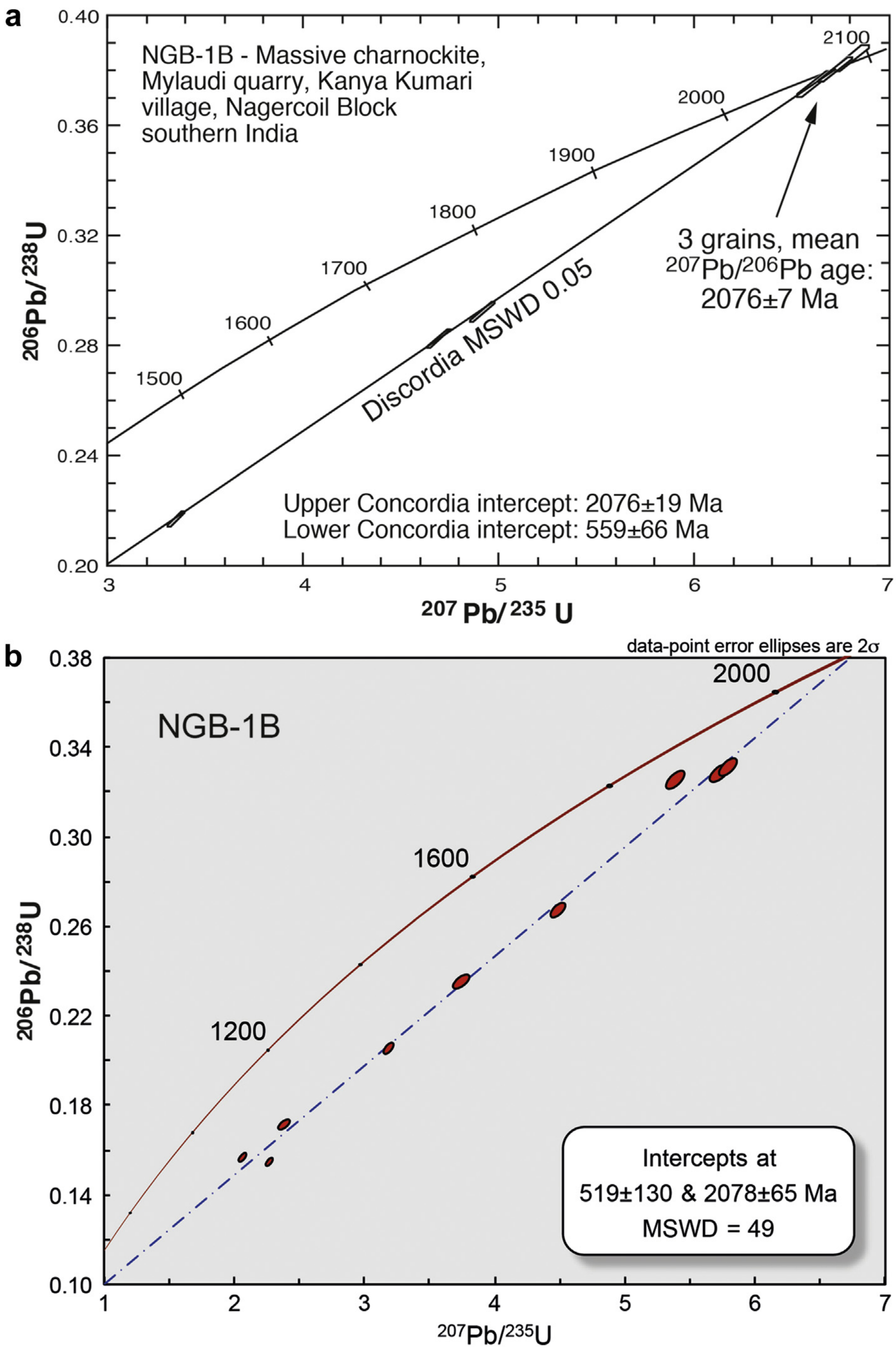

Figure 7. Comparison of SHRIMP II (a) and laser ablation ICP-MS data (b) shown in concordia diagrams for zircon grains from massive charnockite sample NGB-1B, Nagercoil Block, southern India. For analytical data see Tables 1 and 2.

Nagercoil Complex in southernmost India that experienced strong and pervasive granulite-facies metamorphism during the extensive Pan-African event at about 540–580 Ma (Rajesh et al., 2011; Collins et al., 2014). Details on the geology, zircon ages and Nd-Hf isotopic systematics can be found in Kröner et al. (2014), and the SHRIMP analytical data for two charnockite samples are shown in Table 1. The results of the LA-ICP-MS analyses for zircons from the same samples but a different sample mount are presented in Table 2.

First we illustrate and describe some of the zircons and their CL-images. Grain (a) in Fig. 6 is of igneous origin, and some of the original oscillatory zoning is preserved in several domains. However, these magmatic domains exhibit recrystallization as shown by dark grey zones (RC) that overprint the magmatic zonation. Further recrystallization, probably associated with a U-rich fluid phase is represented by almost black very low-luminescent stripes that clearly cut the igneous zonation. The youngest phase in this grain is represented by a dark grey banded phase that surrounds the older domains and is most likely of late metamorphic origin. It is likely that the complex texture of this grain is 3-dimensional, but the interior of the grain is not visible. An ion-microprobe analytical spot on the primary, igneous domain is likely giving the age of magmatic crystallization of this zircon, but a

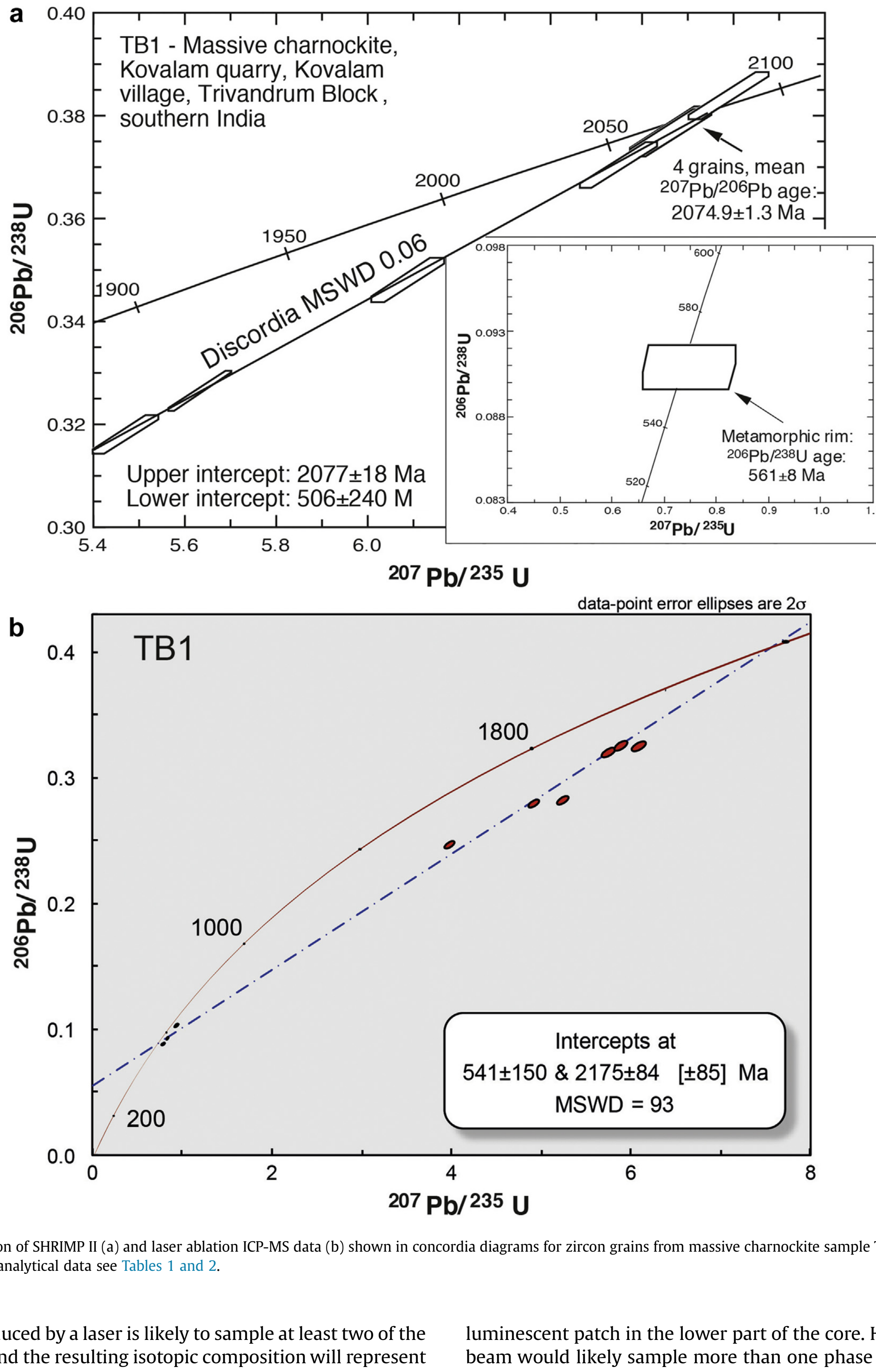

Figure 8. Comparison of SHRIMP II (a) and laser ablation ICP-MS data (b) shown in concordia diagrams for zircon grains from massive charnockite sample TB1, Trivandrum Block, southern India. For analytical data see Tables 1 and 2.

deep pit as produced by a laser is likely to sample at least two of the above phases, and the resulting isotopic composition will represent a mixture between several growth phases and will likely be geologically meaningless.

Grain (b) is also of igneous origin and the original igneous zoning in the light grey core domain is barely visible. This magmatic core has at least three phases of recrystallization as shown by the low-luminescent domain, the medium-grey domain and the highly luminescent patch in the lower part of the core. Here again, a laser beam would likely sample more than one phase of zircon growth. Grain (c) shows a large domain of original magmatic zircon with well-developed oscillatory zoning that is virtually “dissolved” by a tongue of low-luminenscent high-U material, most likely due to the action of a fluid phase. Grain (d) is quite spectacular in that it preserves a large finely oscillatory-zoned magmatic core, surrounded by a broad, fairly homogeneous unzoned rim of likely metamorphic origin. These phases are cut by fluid-induced very low-luminescent replacement material that is also present in small specks within the magmatic phase. This relationship is similar to that shown in Fig. 3a. It is difficult to judge from the CL image whether the magmatic phase continues deep into the grain or whether the interior is mainly composed of recrystallized zircon. In any case, laser-ablation analysis is likely to sample more than one phase.

Finally, there is the problem of dating metamorphic zircons that may contain cores or fragments of inherited material. Fig. 6e illustrates an example of one of the Indian charnockites where near-spherical, multifaceted zircon of metamorphic origin include fragments of older, igneous grains. Since the depth of such inclusions is not known it is possible that laser ablation will sample such material and thus produce an age that will be too old. In addition, as seen in the bottom grain of Fig. 6e, there may be several phases of zircon growth related to a metamorphic event. The complexity of the zircons discussed above underlines the need for an analytical technique that only samples what is seen in CL images.

The effect of mixing of isotopic phases in zircon of the above type is shown by the following examples. Charnockite NGB-1B is a coarse-grained well foliated rock containing large igneous zircons with well rounded terminations. SHRIMP II dating of carefully selected igneous phases with oscillatory zoning yielded three concordant analyses and three variable discordant results (Table 1) that define a discordia line with a lower concordia intercept at 559 ± 66 Ma (Fig. 7a). We interpret this as reflecting magmatic crystallization of the concordant grains at 2067 ± 7 Ma and Pb-loss, probably combined with recrystallization during a pervasive high-grade late Neoproterozoic event in the granulite terrane of southern India (Collins et al., 2014). Zircons from the same sample analyzed by LA-ICP-MS only provided discordant results (Table 2), defining a widely dispersed array of analyses that can be fitted to a similar discordia line as the SHRIMP data (Fig. 7b), but in view of the considerable scatter in these results, both the upper and lower concordia intercept ages have large errors. Nevertheless, the ages obtained by both methods agree within their errors.

A more serious problem is shown by sample TB1, another charnockite from southern India. Again the zircons are clearly of igneous origin but show complex CL patterns. SHRIMP dating (Table 1) yielded four concordant results with a mean $^{207}Pb/^{206}Pb$ age of 2074.9 ± 1.3 Ma (Fig. 8a). Three further discordant results can, as in the previous sample, be explained as a combination of Pb-loss and recrystallization during the high-grade late Pan-African event. In contrast, the LA-ICP-MS analyses are all discordant (Table 2, Fig. 8b) and again scatter considerably. A best-fit line drawn through these data points results in an upper concordia intercept age of 2175 ± 84 Ma that is 100 Ma older than the SHRIMP age and most likely reflects insufficient common Pb correction and/or mixing of several zircon phases that did not all form during magmatic crystallization or metamorphism but at other, unspecified times. This age is clearly erroneous. The lower-intercept age naturally has a large error but is within the range of metamorphic overgrowth as shown in Fig. 8a.

3. Conclusions

There is no doubt that LA-ICP-MS zircon geochronology has considerable advantages over ion-microprobe analysis when isotopically homogeneous crystals or detrital grains are dated because it is fast, cheap and precise because of the large volume ablated. However, we caution against the use of LA-ICP-MS dating of zircons from high-grade metamorphic terranes where CL images reveal complex internal textures resulting from multiple phases of zircon growth and recrystallization. CL images often make it possible to select specific phases for analysis, and as long as these analyses reflect what can be seen in CL images, i.e. they do not deeply penetrate the sample, such as analysis by high-resolution ion microprobe, it may be possible to interpret these data correctly. However, if the zircon is inhomogeneous in three dimensions, then LA-ICP-MS or conventional SIMS analysis samples a mixed composition and is therefore not recommended. The same problem may be encountered with Hf-in-zircon analyses of grains from high-grade terranes with complex internal textures, and some of the published strong variations in initial ε_{Hf} isotopic values may be due to this problem and wrong age assignment.

Acknowledgements

Guangshen Nie and Baoying Zheng of the Beijing SHRIMP Centre prepared the zircon concentrates, Chun Yang prepared a perfect zircon mount, Liqin Zhou provided the high-resolution zircon CL images of Fig. 6, and Jianhui Liu and Zhiqing Yang made sure that SHRIMP II was in excellent operating condition during our analyses. M. Santosh kindly provided the samples from which zircons were extracted, and critical comments of K. Mezger improved the manuscript. This study was partly funded by the German Science Foundation (DFG), grant KR590/94-1 to AK.

Appendix. Analytical procedures

Zircon mounting and cathodoluminescence imaging

Heavy mineral concentrates obtained from the Wiley-table were further purified by panning, and zircons were then handpicked and mounted in epoxy resin together with chips of the zircon standard M257 (Nasdala et al., 2008) in the Beijing SHRIMP Centre, Chinese Academy of Geological Sciences. The mount was ground down and polished so that the zircon interiors were exposed, and zircons were photographed under cathodoluminescence (CL) to enable easy and best location on the mount during SHRIMP and ICP-MS analyses. CL imaging was performed in the Beijing SHRIMP Centre, using a Hitachi S-3000N scanning electron microscope (accelerating voltage 9 kV, beam current 109 mA, pixel time 200; for high-resolution images of Fig. 6 a pixel time of 400 was used).

Isotopic analysis

SHRIMP II zircon analyses were performed in the Beijing SHRIMP Centre, Chinese Academy of Geological Sciences, and the analytical procedures are detailed in Williams (1998) and Kröner et al. (2012). Prior to each analysis, the surface of the analysis site was rastered for 3 min, using the primary beam, to reduce or eliminate surface common Pb. The reduced $^{206}Pb/^{238}U$ ratios were normalized to 0.09101, which is equivalent to the adopted age of 561.3 Ma for standard M257. Pb/U ratios in the unknown samples were corrected using the ln(Pb/U)/ln(UO/U) relationship as measured in M257 and as outlined in Compston et al. (1992) and Nelson (1997). The 1σ error in the ratio $^{206}Pb/^{238}U$ during analysis of all standard zircons during this study was 1.19%. Primary beam intensity was 5.2 nA, and a Köhler aperture of 100 μm diameter was used, giving a slightly elliptical spot size of about 30 μm. Peak resolution (at 1% peak height) was 5010, enabling clear separation of the ^{208}Pb-peak from the HfO peak. Analyses of samples and standards were alternated to allow assessment of Pb^+/U^+ discrimination. Raw data reduction and error assessment followed the method described by Nelson (1997). Common Pb corrections were applied using the ^{204}Pb-correction method and assuming the isotopic composition of Broken Hill, because common Pb is thought to be surface-related (Kinny, 1986). The analytical data are presented in Table 1. Errors given on individual analyses are based on counting statistics and are at the 1σ level and include the uncertainty of the standard added in quadrature. Errors for pooled analyses are at 2σ.

The ICP-MS analyses were carried out on an Agilent 7500a instrument, connected to a Geolas-193 UV laser ablation system in the State Key Laboratory of Continental Dynamics, Northwest University, Xi'an. A 20 μm spot diameter was used with a laser repetition rate of 6 Hz. The detailed analytical procedures are described in Liu et al. (2007), and standards 91500 and GJ were used for calibration. The analytical results are given in Table 2.

References

Andersen, T., 2002. Correction of common lead in U-Pb analyses that do not report ^{204}Pb. Chemical Geology 192, 59–79.
Ashwal, L.D., Tucker, R.D., Zinner, E.R., 1999. Slow cooling of deep crustal granulites and Pb-loss in zircon. Geochimica et Cosmochimica Acta 63, 2839–2851.
Cherniak, D.J., Watson, E.B., 2001. Pb diffusion in zircon. Chemical Geology 172, 5–24.
Collins, A.S., Clark, C., Plavsa, D., 2014. Peninsular India in Gondwana: the tectonothermal evolution oft he Southern Granulite Terrain and its Gondwanan counterparts. Gondwana Research 25, 190–203.
Compston, W., Williams, I.S., Kirschvink, J.L., Zhang, Z., Ma, G., 1992. Zircon U-Pb ages for the Early Cambrian time scale. Journal of the Geological Society of London 149, 171–184.
Connelly, J.N., 2001. Degree of preservation of igneous zonation in zircon as a signpost for concordancy in U-Pb geochronology. Chemical Geology 172, 25–39.
Corfu, F., 2007. Multistage metamorphic evolution and nature of the amphibolites-granulite facies transition in Lofoten-Vesterålen, Norway, revealed by U-Pb in accessory minerals. Chemical Geology 241, 108–128.
Corfu, F., 2013. A century of U-Pb geochronology: the long quest towards concordance. Geological Society of America Bulletin 125, 33–47.
Corfu, F., Heaman, L.M., Rogers, G., 1994. Polymetamorphic evolution of the Lewisian complex, NW Scotland, as recorded by U-Pb isotopic compositions of zircon, titanite and rutile. Contributions to Mineralogy and Petrology 117, 215–228.
Cottle, J.M., Horstwood, M.S.A., Parrish, R.R., 2009. A new approach to single shot laser ablation analysis and its application to in situ Pb/U geochronology. Journal of Analytical Atomic Spectrometry 24, 1355–1363.
Dong, C.Y., Wan, Y.S., Xu, Z.Y., Liu, D.Y., Yang, Z.S., Ma, M.Z., Xie, H.Q., 2013. Khondalites of the late Paleoproterozoic in the Daqingshan area, North China Craton: SHRIMP zircon U–Pb dating. Science in China, Series D 56, 115–125.
Flowers, R.M., Schmitt, A.K., Grove, M., 2010. Decoupling of U-Pb dates from chemical and crystallographic domains in granulite facies zircon. Chemical Geology 270, 20–30.
Gehrels, G.E., Valencia, V.A., Ruiz, J., 2008. Enhanced precision, accuracy, efficiency, and spatial resolution of U-Pb ages by laser ablation–multicollector–inductively coupled plasma–mass spectrometry. Geochemistry, Geophysics, Geosystems 9, Q03017.
Geisler, T., Schaltegger, U., Tomaschek, F., 2007. Re-equilibration of zircon in aqueous fluids and melts. Elements 3, 43–50.
Horn, I., Rudnick, R.L., McDonough, W.F., 2000. Precise elemental and isotope ratio determination by simultaneous solution nebulization and laser ablation- ICP-MS: application to U-Pb geochronology. Chemical Geology 164, 281–301.
Jackson, S.E., Pearson, N.J., Griffin, W.L., Belousova, E.A., 2004. The application of laser ablation–inductively coupled plasma–mass spectrometry to in situ U-Pb zircon geochronology. Chemical Geology 211, 47–69.
Kinny, P.D., 1986. 3820 Ma zircons from a tonalitic Amitsoq gneiss in the Godthab district of southern West Greenland. Earth and Planetary Science Letters 79, 337–347.
Kooijman, E., Upadhyay, D., Mezger, K., Raith, M.M., Berndt, J., Srikantappa, C., 2011. Response of the U-PB chronometer and trace elements in zircon to ultrahigh-temperature metamorphism: the Kadavur anorthosite complex, southern India. Chemical Geology 20, 177–188.
Košler, J., Fonneland, H., Sylvester, P., Tubrett, M., Pedersen, R.-B., 2002. U-Pb dating of detrital zircons for sediment provenance studies—a comparison of laser ablation ICP-MS and SIMS techniques. Chemical Geology 182, 605–618.
Krogh, T.E., Davis, G.L., 1974. Alteration in zircons with discordant U-Pb ages. In: Carnegie Institution Washington, Yearbook, vol. 73, pp. 560–567.
Krogh, T.E., Davis, G.L., 1975. Alteration in zircons and differential dissolution of altered and metamict zircon. In: Carnegie Institution Washington, Yearbook, vol. 74, pp. 619–623.
Kröner, A., 2001. The Mozambique belt of East Africa and Madagascar: significance of zircon and Nd model ages for Rodinia and Gondwana supercontinent formation and dispersal. South African Journal of Geology 105, 151–167.
Kröner, A., Compston, W., Williams, I.S., 1989. Growth of early Archaean crust in the Ancient Gneiss Complex of Swaziland as revealed by single zircon dating. Tectonophysics 161, 271–298.
Kröner, A., Santosh, M., Wong, J., 2012. Zircon ages and Hf isotopic systematics reveal vestiges of Mesoproterozoic to Archaean crust within the late Neoproterozoic–Cambrian high-grade terrain of southernmost India. Gondwana Research 21, 876–886.
Kröner, A., Rojas-Agramonte, Y., Kehelpannala, K.V.W., Zack, T., Hegner, E., Wong, J., Barth, M., 2013. Age, Nd–Hf isotopes, and geochemistry of the Vijayan Complex of eastern and southern Sri Lanka: a Grenville-age magmatic arc of unknown derivation. Precambrian Research 234, 288–321.
Kröner, A., Santosh, M., Hegner, E., Liu, S., Geng, H., Wong, J., Shaji, E., 2014. Zircon ages and Nd-Hf isotopic systematics for Palaeoproterozoic igneous rocks of the Trivandrum Block, southern India. Gondwana Research (in revision).
Kusiak, M.A., Whitehouse, M.J., Wilde, S.A., Nemchin, A., Clark, C., 2013. Mobilization of radiogenic Pb in zircon revealed by ion imaging: Implications for early Earth geochronology. Geology 41, 291–294.
Lee, J.K.W., Williams, I.S., Ellis, D.J., 1997. Pb, U and Th diffusion in natural zircon. Nature 390, 159–161.
Liu, X., Gao, S., Diwu, C., Yuan, H., Hu, Z., 2007. Simultaneous in-situ determination of U–Pb age and trace elements in zircon by LA-ICP-MS in 20 μm spot size. Chinese Science Bulletin 52, 1257–1264.
Ma, M., Wan, Y., Santosh, M., Xu, Z., Xie, H., Dong, C., Liu, D., Guo, C., 2012. Decoding multiple tectonothermal events in zircons from single rock samples: SHRIMP zircon U–Pb data from the late Neoarchean rocks of Daqingshan, North China Craton. Gondwana Research 22, 810–827.
McFarlane, C.R.M., Connelly, J.N., Carlson, W.D., 2005. Intracrystalline redistribution of Pb in zircon during high-temperature metamorphism. Chemical Geology 217, 1–28.
Mezger, K., Krogstad, E.J., 1997. Interpretation of discordant U-Pb zircon ages: an evaluation. Journal of Metamorphic Geology 15, 127–140.
Möller, A., O'Brien, P.J., Kennedy, A., Kröner, A., 2003. Linking growth episodes of zircon and metamorphic textures to zircon chemistry: an example from the ultrahigh-temperature granulites of Rogaland (SW Norway). Geological Society, London, Special Publications 220, 65–81.
Moser, D.E., Davis, W.J., Reddy, S.M., Flemming, R.L., Hart, R.J., 2009. Zircon U-Pb strain chronometry reveals deep impact triggered flow. Earth and Planetary Science Letters 277, 73–79.
Moser, D.E., Cupelli, C.L., Barker, I.R., Flowers, R.M., Bowman, J.R., Wooden, J., Hart, J.R., 2011. New zircon shock phenomena and their use for dating and reconstruction of large impact structures revealed by electron nanobeam (EBSD, CL, EDS) and isotopic U-Pb and (U-Th)/He analysis of the Vredefort dome. Canadian Journal of Earth Sciences 48, 117–139.
Nasdala, L., Hofmeister, W., Norberg, N., Mattinson, J.M., Corfu, F., Dàrr, W., Kamo, S.L., Kennedy, A.K., Kronz, A., Reiners, P.W., Frei, D., Kosler, J., Wan, Y., Gàtze, J., Hâger, T., Kràner, A., Valley, J.W., 2008. Zircon M257-a homogeneous natural reference material for the ion microprobe U-Pb analysis of zircon. Geostandards and Geoanalytical Research 32, 247–265.
Nelson, D.R., 1997. Compilation of SHRIMP U-Pb Zircon Geochronology Data, 1996. Geological Survey of Western Australia, Record 1997/2, 189 pp.
Patchett, P.J., Samson, S.D., 2011. Ages and growth of the continental crust from radiogenic isotopes. In: Holland, H.D., Turekian, K.K. (Eds.), Radioactive Geochronometry. Academic Press, Elsevier Publishers, Amsterdam, pp. 223–250.
Pidgeon, R.T., Nemchin, A.A., Hitchen, G.J., 1998. Internal structures of zircons from Archaean granites from the Darling Range batholith: implications for zircon stability and the interpretation of zircon U–Pb ages. Contributions to Mineralogy and Petrology 132, 288–299.
Rajesh, H.M., Santosh, M., Yoshikura, S., 2011. The Nagercoil cahrnockite: a magnesian, calcic to calc-alkalic granitoid dehydrated during Na granulite-facies metamorphic event. Journal of Petrology 52, 375–400.
Wan, Y.S., Liu, D.Y., Dong, C.Y., Liu, S.J., Wang, S.J., Yang, E.X., 2011. U–Th–Pb behavior of zircons under high-grade metamorphic conditions: a case study of zircon dating of meta-diorite near Qixia, eastern Shandong. Geoscience Frontiers 2, 137–146.
Williams, I.S., 1998. U–Th–Pb geochronology by ion microprobe. In: McKibben, M.A., Shanks III, W.C., Ridley, W.I. (Eds.), Applications of Microanalytical Techniques to Understanding Mineralizing Processes. Reviews in Economic Geology, vol. 7, pp. 1–35.
Williams, I.S., Compston, W., Black, L.P., Ireland, T.R., Foster, J.J., 1984. Unsupported radiogenic Pb in zircon: a case of anomalously high Pb-Pb, U-Pb and Th-Pb ages. Contributions to Mineralogy and Petrology 88, 322–327.
Xia, X., Sun, M., Zhao, G., Li, H., Zhou, M., 2004. Spot zircon U-Pb isotope analysis by ICP-MS coupled with a frequency quintuplet (213 nm) Nd-YAG laser system. Geochemical Journal 38, 191–200.